ARTICLES

Characterization and Preparation of Chained Si Species in Zeolite Supercages

Katsumi Tanaka,*,†,‡ Cheow-Keong Choo,† Yuhko Komatsu,‡,|| Kohji Hamaguchi,‡,⊥ Masahiro Yamaki,‡,# Tomonori Itoh,‡,^ Takehiko Nishigaya,‡,+ Rhouhei Nakata,† and Katsunao Morimoto§

Department of Human Communication, The University of Electro-Communications, 1-5-1 Chofu Tokyo 182-8585, Japan, Graduate School of Electronic Engineering, The University of Electro-Communications, 1-5-1 Chofu Tokyo 182-8585, Japan, and ANELVA Corporation, 8532-28 Narusawa, Minamitsuru-gun Yamanashi, 401-0397, Japan

Received: April 17, 2003; In Final Form: December 16, 2003

Chained Si species were synthesized in Y-type zeolite supercages by the reaction with phenylsilane ($PhSiH_3$) at 423 K. The preparation process was studied with the infrared spectra, and the prepared Si species were characterized with X-ray photoelectron spectroscopy (XPS), photoluminescence (PL) spectra, and ultraviolet absorption spectra. The initial sticking reaction of SiH_x species to zeolite framework was studied with a temperature-programmed desorption experiment on the deuterium-exchanged zeolite using a quadrupole mass spectrometer. Benzene molecules composed selectively with d_1 species (C_6H_5D) were desorbed with hydrogen molecules at 360−380 K; concurrently, hydroxyl groups in supercages disappeared. These results imply that the initial grafting reaction of Si species to a HY−zeolite framework proceeds through the thermal reaction of $PhSiH_3$ with hydroxyl groups in supercages at 298 K to yield [O]−SiH_3 and benzene. The formed [O]−SiH_x species were characterized with infrared spectra as a function of reaction temperature. The wavenumbers shift in Si−H species was explained by the thermal conversion of [O]−SiH_3 (2180 cm^{-1}) to $[O]_2$−SiH_2 (2208 cm^{-1}) and $[O]_3$−SiH (2270 cm^{-1}). The reaction of $PhSiH_3$ molecules with hydroxyl groups in supercages at 423 K suggests the propagation of Si species finally to yield $[O]_2$−Si_xH_y. The successive propagation reaction with $PhSiH_3$ yielded Si species with Si 2p XPS signals at 101.4 and 102.3 eV, which could be assigned to polysilane families. The quantitative XPS analysis implied that polysilane families with about 30 Si atoms were produced in a zeolite super cage. The zeolite pressed between metal barrels showed intense PL spectra peaked at 340 (3.6 eV) and 460 nm (2.7 eV). The peak intensities diminished considerably with treatment with oxygen gas at 573 K for 48 h, which caused the selective enhancement of X-ray diffraction intensity at around $2\theta = 6°$, characteristic of a zeolite (111) face. These results induce that surface contaminants such as organic compounds can be removed by the oxygen treatment as well as the zeolite crystallinity is improved by the decrease of oxygen vacancies. Chained Si species in zeolite supercages showed intense PL spectra at around 4 eV. The Si species can be extracted in hexane at 298 K, and the extracted species also showed redshifted intense PL spectra peaked at 4.07 eV. The broad UV spectra due to the polysilane backbone structure was detected at 220−280 nm. It is concluded that polysilane families are formed in zeolite supercages and absorb excitation photon energy and relax to show PL characteristic to the Si backbone structure.

Introduction

Nanometer-sized particles, especially silicon, raise much interest in applications not only to electronic devices but also to optoelectronic devices. In fact, photoluminescence spectra for silicon nanoparticles have been widely studied to apply nanosized silicon to optoelectronic devices.[1−12] Silicon clusters composed of almost all surface atoms become relatively stable because they have corresponding compact structures with less number of dangling bonds.[13] For example, silicon nanoparticles reveal lower oxidation reaction rates as their diameters decrease.[14] The activity of silicon cluster ions with oxygen gas is lower than Si(111)7 × 7 surface by 1−4 orders of magnitude.[15] On the other hand, the melting points of silicon nanocrystals drop drastically with the crystal radii below 10 nm.[16] Silicon clusters below 50 Si atoms reveal no structure change with annealing, whereas the conformation of structural isomers is effected.[15] The termination of silicon species is also significant to stabilize the surface dangling bonds.[18,19]

* Author to whom correspondence may be addressed. E-mail: tanaka@hc.uec.ac.jp.
† Department of Human Communication, The University of Electro-Communications.
‡ Graduate School of Electronic Engineering, The University of Electro-Communications.
§ ANELVA Corporation.
|| Present Address: Epson.
⊥ Present Address: Hitachi Kasei.
Present Address: TDK.
^ Present Address: Nagano Electronic.
+ Present Address: NKK.

10.1021/jp035043r CCC: $27.50
Published on Web 02/03/2004

So far, some challenges have been tried to make sub-nanosized clusters,[20−24] semiconductors,[25−30] polymers,[31−33] and catalysts[34,35] in zeolite pores. Zeolites are inorganic aluminosilicate materials composed of three-dimensional pore structures with different sizes. There are many types of zeolites with different pore structures.[36] The use of zeolites for molecular recognition and separation has been one of the key targets in the field of industrial chemistry. The oriented growth of zeolites as well as zeolite membranes is also possible.[37−39] However, an interest on zeolites seems to lie in the use of pores as a vessel for the occlusion chemistry and for the synthesis of dimension-defined materials.[40] The synthesis of confined clusters in the pores seems to be indirectly brought about by the formation of Na_4 clusters in sodalite cages of zeolites.[41−43] It is also based on the fact that the Na ion exchanged zeolite is most stable among faujasite zeolites and Na ions are mainly located in sodalite cages of FAU zeolites.[44−46] While the one-dimensional channels of $AlPO_4$-5 molecular sieves also have been applied to significant carbon nanotube synthesis[47] as well as an optical second harmonic generation.[48] The inner surface of a molecular sieve $AlPO_4$-5 is very inert, and it is difficult to make strong chemical bonds with functional groups since no hydroxyl group exists. In this sense, not only the zeolite but also the molecular sieve inclusion chemistry gathers much interest.[49] One of the aims of our study is to synthesize intrazeolitic Si species for photoluminescence. We have tried to include Si clusters in the $AlPO_4$-5 pores by thermal diffusion.[50−52] Although encapsulated II−VI group semiconductor clusters in zeolites have been widely studied, only few works have been carried out on silicon clusters encapsulated in zeolite pores.[53,54] Recently silicon nanoclusters with an average value of 12 ± 2 Si/cluster have been successfully encapsulated in zeolite Y cavities through zeolite framework OH groups.[55,56] The encapsulated silicon clusters are air stable and exhibit a room-temperature photoluminescence in the green-yellow region.

In the present paper, we wish to report a new approach using the step-by-step Si chain extension reaction using volatile compounds such as phenylsilane ($PhSiH_3$). This molecule is small enough to reach Y-type zeolite supercages through the entrance of 12-membered rings with diameter of 0.74 nm but big enough not to reach the sodalite cages. Therefore it is expected that the Si−Si bond length can be controlled in zeolite pores after releasing benzene through the thermal reactions. How the Si−Si chain continues in zeolite pores, linear or branched, is an interesting objective to be studied. Ladderlike structures derived from *syn*-tricyclooctasilane molecules are assumed for the structure of intrazeolitic Si clusters formed by chemical vapor deposition (CVD) of disilane.[56] The initial grafting reaction of Si species to the zeolite framework is also an interesting process to be studied. It is significantly reported in this study that the intrazeolitic Si species can be extracted with an organic solvent and are characterized with ultraviolet and photoluminescence spectra. The fact will raise a strong motivation to the application of the intrazeolitic species to optoelectronic devices because it can make the handling possible in solution media for their related processes.

Experimental Section

Faujasite zeolite mainly used was the HY zeolite (Tosoh Corp.) with a SiO_2/Al_2O_3 ratio of 5.6 and surface area of 570 $m^2\ g^{-1}$, in which 68% of Na ions of the starting NaY (surface are of 700 $m^2\ g^{-1}$) had been changed into H ions. The X-ray diffraction (XRD) pattern of the HY zeolite powder showed the crystal structure similar to the Na−Y zeolite. The powder was pressed at 150 kg cm^{-2} between two metal barrels. The amount of the pellet for infrared (IR) and photoluminescence (PL) was 0.1 and 0.5 g, respectively. The pellet for IR experiments was put on a glass-made holder inside a Pyrex-made infrared cell with diameter of 30 mm. The pellet was treated with 13.3 hPa (10.0 Torr) of oxygen gas in the cell at 673 K, and oxygen gas was changed several times. It was evacuated at 673 K for dehydration by heating with a ribbon heater put outside the cell after the pellet was transferred to the heating area by a magnet. The temperature difference between the holder and the ribbon heater was calibrated. The pellet inside the infrared cell was evacuated below 1×10^{-4} Pa through a stop-valve connected to a ultrahigh vacuum system, which was equipped with an ion vacuum gauge, quadrupole mass spectrometer (M-QA200TS: ANELVA), and some gas manifolds for organic reagents. The overall system was evacuated with a 150 L s^{-1} turbo molecular pump back supported with a 100 L min^{-1} rotary pump. The base pressure of the system was below 1×10^{-6} Pa. The H−D exchanged zeolite was made as follows. The oxygen gas treated pellet was reacted with 6.65 hPa (5.0 Torr) of deuterium water (D_2O purity 99.9%) at 298 K several times in the IR cell and finally evacuated at 673 K for 30 min. The cease of H−D exchange was ascertained by the complete conversion of O−H into O−D groups with infrared spectra. IR spectra were recorded at 298 K through KBr windows as subtraction spectra referenced to a fresh zeolite. A Fourier transform IR spectrometer (Perkin-Elmer FT-IR: Model 1600) was used at 256 scans. The phenylsilane liquid ($PhSiH_3$: Shin-Etsu Chemicals, purity >99.5%) was reserved in glass vessels and was degassed at several freeze−pump−thaw cycles. The dosed amount of phenylsilane for IR and PL experiments was 0.133 hPa (0.1 Torr) and 6.65 hPa (5.0 Torr), respectively.

X-ray photoelectron spectroscopic (XPS) data were recorded with Al Kα radiation (1486.6 eV) at pass energy of 50 eV in an ESCA chamber (VG-ESCA Lab 5). The oxygen-treated zeolite and the $PhSiH_3$-reacted zeolite were exposed to air when they were transferred from the $PhSiH_3$ reaction chamber to the ESCA chamber. No further treatment was carried out on the samples except evacuation in the ESCA chamber. PL spectra of the Si species were recorded at 298 K in situ with a multichannel photodetector (Hamamatsu photonics, PMA-11, C7473-36). PL spectra were excited with a pulsed 266-nm laser (FHG of Nd−YAG laser: Continuum, Surelite-10) at 10 Hz with a laser intensity far below the ablation threshold of zeolite. The pellet of 0.5 g for PL experiments was treated with 1013 hPa (1atm) of oxygen gas flowed at 573 K for 48 h and was transferred to a sample holder made of tantalum (Ta) in a 6-way cube, which had been connected to the evacuation system mentioned above. It was finally evacuated at 673 K for 30 min. For extraction of Si species in organic solvent, the zeolite sample was evacuated at 673 K for 30 min and was dipped in a water-free hexane solution at 298 K overnight. The solution was separated from zeolite powder with a paper filter. Si species extracted in hexane solvent was studied with UV/VIS spectrophotometer (JASCO Ubest-30).

Results and Discussion

Effects of oxygen treatment on a pressed zeolite were studied with PL spectra and XRD. As shown in Figure 1, the pressed zeolite showed the intense PL peak at 460 nm (2.7 eV) with shoulders at 415 nm (3.0 eV) and 340 nm (3.6 eV). The PL species at 2.7 and 3.6 eV are typical, which will be clear in Figure 9. The PL intensity decreased after the treatment with oxygen flowed at 573 K overnight. The PL intensity was almost

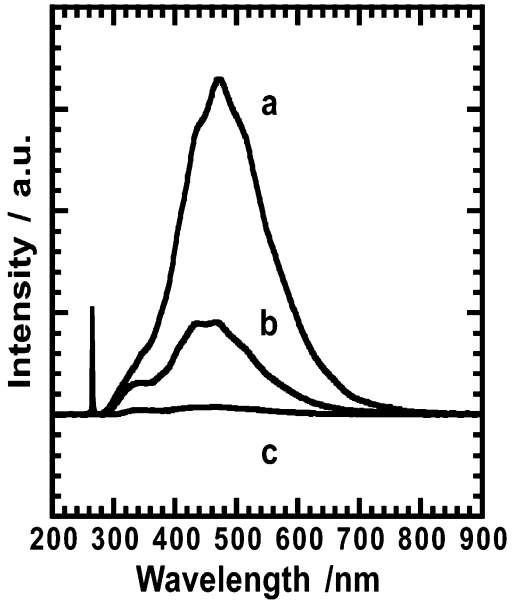

Figure 1. PL spectra of (a) a pressed 0.5-g HY zeolite, (b) treated with 1013 hPa oxygen at 573 K for 24 h, (c) and 48 h.

negligible with the oxygen treatment for 48 h but remained a little as shown in Figure 9. The reason is mentioned later. The surface of pressed zeolite will be covered with contaminants such as organic molecules supplied from metal barrels. It is also obvious that there are lots of defect sites such as oxygen vacancies in zeolites because of the crystalline imperfection. At least two species showing typical PL peaks diminish their intensities with the oxygen treatment. The fact suggests two possibilities; that is, contaminants such as organic molecules are removed, and oxygen vacancies are filled with. On silica-based materials, PL peaks have been observed at 1.93, 2.37, and 2.8 eV, which can be assigned to nonbonding oxygen hole centers in bulk, hydrogen-related Si−H species, and triplet-to-singlet transition in self-trapped excitons in a bulk silica system, respectively.[57−60] The PL component on zeolite at 2.7 eV will be assigned to the one on silica. However, the PL intensity was drastically suppressed after the oxygen treatment. The fact strongly suggests that oxygen vacancies are responsible for the PL species at 2.7 eV. The PL at 3.6 eV will be due to uncontrolled organic impurities as reported.[61] The organic molecules were studied with IR experiments. If hydrocarbon species are present, the stretching frequency of CH_x species should be detected. However, no such species was detected. One can imagine that a detection limit exists as the threshold of species with IR. It is easily understood that PL is much more sensitive than IR.

Figure 2 shows the XRD data of the pressed H−Y zeolite. The typical reflection peaks can be seen at (111), (220), (311), (333), (440), (533), and (555) faces. When the pressed zeolite was oxidized with oxygen at 573 K for 48 h, a drastic change was observed on the XRD data. As shown in Figure 2, the intensity of XRD peaks detected at lower degree of 2θ such as (111), (220), (311), and (331) was drastically increased. This result implies that the reflection strength is increased at the crystal faces with longer interplane distance in the zeolite crystal structure. It will be associated with the fact that the crystallinity is increased as oxygen vanancies are removed.

Temperature-programmed desorption (TPD) experiments were carried out to elucidate the initial sticking reaction of $PhSiH_3$ to the zeolite framework. The zeolite sample was used, whose O−H groups had been exchanged into O−D groups.

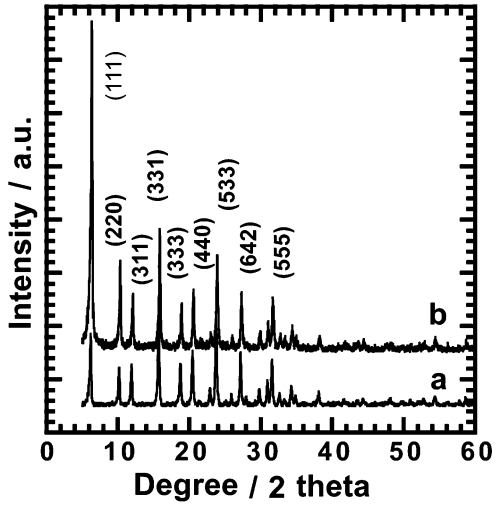

Figure 2. XRD spectra (a) of the pressed 0.5-g zeolite and (b) of the zeolite treated with 1013 hPa oxygen for 48 h.

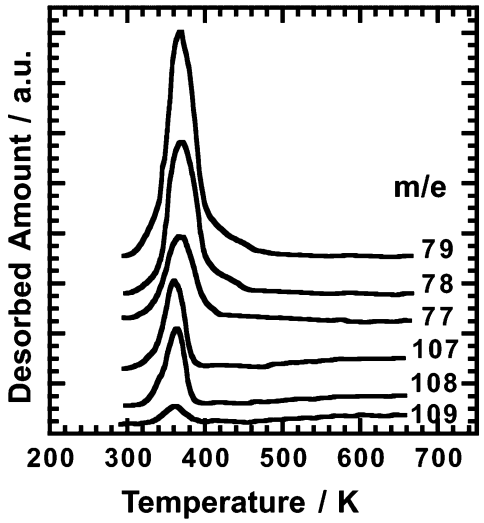

Figure 3. TPD spectra of desorbed species formed in the reaction of $PhSiH_3$ with deuterated 0.1-g HY zeolite (DY zeolite) at 298 K. The zeolite was exposed to 0.665 hPa (0.5 Torr) at 298 K for 30 min, then followed by evacuation at the same temperature. Note that *m*/*e* ratios of 79 and 109 correspond to C_6H_5D (benzene-d_1) and $PhSiH_2D$ (phenylsilane-d_1), respectively. Considering fragmentation pattern of benzene, almost 100% of benzene are d_1-species.

They were converted to O−D groups at 2645, 2600, and 2560 cm^{-1}. The zeolite was evacuated at 673 K for 1 h. Phenylsilane (0.133 hPa, 0.1 Torr) was adsorbed on the H−D-exchanged zeolite at 298 K for 30 min, then it was evacuated at the same temperature. The sample was evacuated while elevating the temperature at 5 K min^{-1}, and desorbed gases were analyzed with Q-mass. Figures 3 and 4 show the TPD results. Species with the mass-to-charge ratio of 2, 3, 4, 77, 78, 79, 107, 108, and 109 were typical, and the latter three signals disappeared with lower desorption maximum by about 5 K than the other species. The result implies that (i) $PhSiH_3$ desorbs prior to formed benzene at lower temperature, (ii) desorbed benzene is composed of almost 100% benzene-d_1 (C_6H_5D), which can be assigned due to the fragmentation pattern, and (iii) H_2 and HD is desorbed. A TPD experiment was carried out on the zeolite after adsorbing benzene at 298 K. The benzene desorption maximum was observed at the same TPD peak for benzene as in Figure 3. Therefore it seems that $PhSiH_3$ is decomposed even at 298 K and formed benzene desorbs at 373 K. It is noted that no C−H group is detected on the $PhSiH_3$- reacted zeolite surface

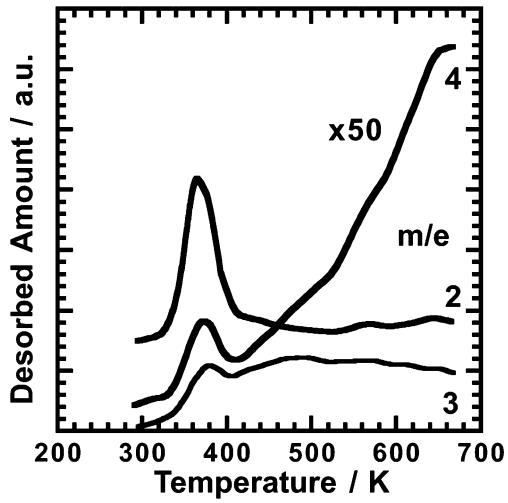

Figure 4. TPD spectra of desorbed species formed in the reaction of $PhSiH_3$ with deuterated HY zeolite (DY zeolite) at 298 K. Experimantal conditions were the same as in Figure 3. Mass-to-charge ratios (*m*/*e*) of 2, 3, and 4 correspond to H_2, HD, and D_2, respectively.

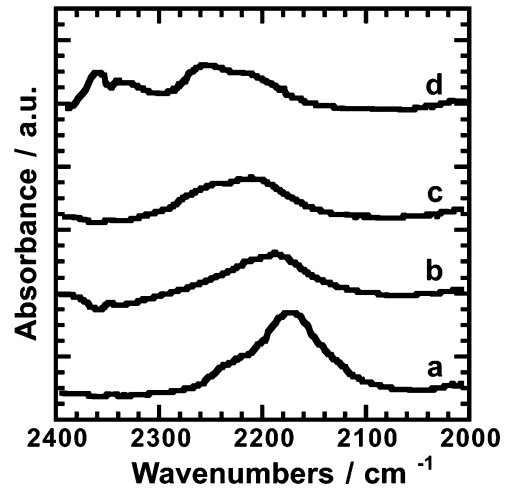

Figure 5. IR spectra of Si−H groups on the 0.1-g HY zeolite after adsorbing 0.133 hPa (0.1 Torr) $PhSiH_3$ at 298 K for 30 min then followed by evacuation at 373 K (a), 473 K (b), 573 K (c), and 673 K (d) each for 30 min. The spectra were recorded at 298 K.

after evacuation at 373 K. Therefore it is concluded that benzene will be formed by the following reaction

$$PhSiH_3 + [O]-D \rightarrow [O]-SiH_x + Ph-D + yH_2 \quad (1)$$

Here [O] represent oxygen ions in the zeolite framework. The location of adsorbed benzene has been studied. One site is 0.27 nm apart from the $S_{II}Na$ ion, and the center of the molecule is on the cube diagonal. The second site is the 12-ring window between adjacent supercages.[62,63] The diffusion ability of benzene in NaY is smaller than NaX zeolite by 2 orders of magnitude with diffusion activation energy of 141 $kJ \cdot mol^{-1}$.[64] In eq 1, hydroxyl groups are changed into $O-SiH_x$ species. Then the effective inner diameter of the zeolite supercages does not change so much that benzene molecules are probably possible to situate the adsorption sites. Hydrogen exchange reaction proceeds between benzene and hydroxyl group in zeolite.[65] The exchange reaction will be negligible in our experiments since hydroxyl groups have been exchanged into $O-SiH_x$ species.

Figure 5 shows spectra in the Si−H stretching region after evacuating the sample at 373, 473, 573, and 673 K. Phenylsilane (0.133 hPa, 0.1 Torr) was adsorbed on the 673-K evacuated zeolite at 298 K for 30 min. The system was evacuated at 298 K, and then the sample temperature was elevated gradually. This experiment was carried out to study the initial sticking reaction of $PhSiH_3$ to the zeolite framework. An infrared spectrum of $PhSiH_3$ in the gas phase was recorded and was found to have a very sharp but a weak signal at 2165 cm^{-1}. The signal disappeared completely after evacuating the system at 298 K. Therefore Si−H species observed in Figure 5 clearly originate from adsorbed species. At 373 K, the species appeared at 2230 cm^{-1} in addition to an appearance at 2180 cm^{-1}. Two peaks were detected at 2208 and 2270 cm^{-1} at 573 K, while the latter species was selectively observed at 673 K. These results infer that three SiH_x species will be present at 2180, 2208, and 2270 cm^{-1} and that the former species changes into the second and the last species as the temperature increases. On silicon single crystals, Si−H stretching frequencies for surface monohydride (Si−H) and dihydride (SiH_2) are observed at 2090 and 2114 cm^{-1}, respectively,[66] while Si−H species on the H_2O exposed porous silicon surface shows the wavenumbers shift from 2090 to 2100 cm^{-1} with temperature rise.[67] According to the assignment of Si−H stretching frequencies of the $HSi-Si_{3-n}O_n$ ($n = 0-3$) bonding configurations, the four bands at respective *n* value are separated by 50 cm^{-1}.[68] A large wavenumbers shift is also observed on the oxidized Si−H species, that is, Si−H and O_xSi-H species are observed in porous silicon at 2091 and 2269 cm^{-1}, respectively.[69] It is also known that the Si−H bond reveals a similar wavenumbers shift when Si is bonded to N atoms with higher electronegativity as well as O atoms.[70] In summary, it has been reported that O_3SiH, O_2SiH_2, and $OSiH_3$ species show Si−H stretching frequency at 2250−2260, 2206, and 2200 cm^{-1}, respectively.[71−74] As a conclusion, 2270, 2206, and 2180 cm^{-1} in Figure 5 will be assigned to the O_3SiH, O_2SiH_2, and $OSiH_3$ species, respectively. The following initial sticking reaction of the adsorbed SiH_x species will be most reasonable in our system

$$[O]-SiH_3 \rightarrow (373\ K) \rightarrow [O]_2-SiH_2 \rightarrow (573\ K) \rightarrow [O]_3-SiH \quad (2)$$

Here [O] and suffix *n* of $[O]_n$ represent the zeolite framework oxygen atom and the number, respectively. In our system, it was difficult to find an optimum condition to detect the $[O]_2-SiH_2$ species selectively. Hydrogen molecules must be formed during reaction 2. Deuterium molecules continued to desorb at elevating the sample temperature as shown in Figure 4. The origin is surely O−D groups in zeolite; however, the signal is very weak. If desorption of D atoms from O−D groups occurs concurrently with that of H atoms in reaction 2, desorption of HD molecules will be reasonable. In fact, the signal of mass number 3 (HD) continues to increase at temperatures over 400 K. The fact strongly suggests the validity of reaction 2. CH_3M species (M = Zn, Cd) are found to be anchored by CVD via the metal center to zeolite framework oxygens both at site II (four-membered ring) and III (six-membered ring).[75] There are four- and six-membered rings composed of a Si−O−Si bond unit in supercages. The $[O]-SiH_3$ and $[O]_2-SiH_2$ species can be formed in both the four- and six-membered rings, while $[O]_3-SiH$ species will be formed only in six-membered rings.

When the zeolite was reacted with $PhSiH_3$ at 423 K and was evacuated at the same temperature, Si−H species were peaked at around 2210 cm^{-1} with a shoulder at 2260 cm^{-1} as shown in Figure 7. At the same time only the hydroxyl groups at 3680 cm^{-1} disappeared in the reaction with phenylsilane as shown in Figure 8. It is noted that $PhSiH_3$ was adsorbed on zeolite at

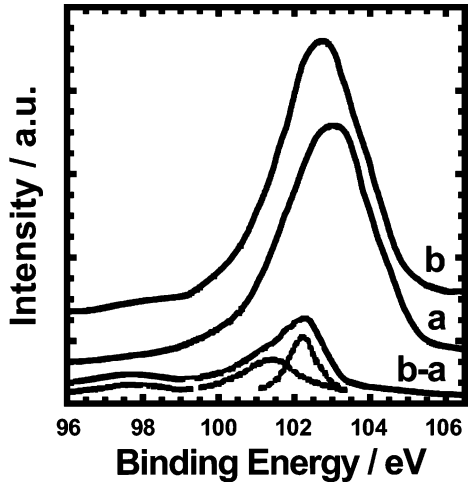

Figure 6. XPS spectra of Si 2p signals of the zeolite (a), the $PhSiH_3$ reacted zeolite (b), and the subtracted spectrum (b−a). Binding energy values are referenced to C 1s at 284.4 eV and O 1s at 531.6 eV.

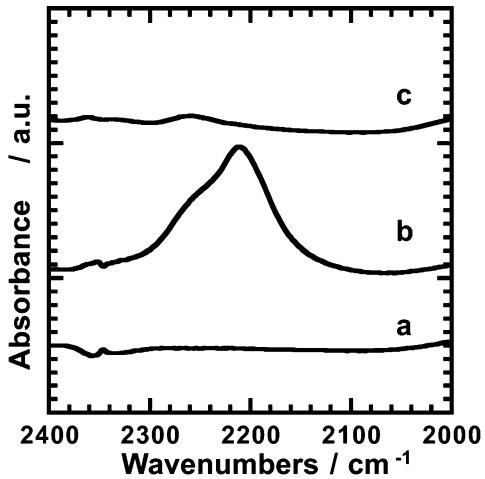

Figure 7. IR spectra of Si−H stretching frequency region on the oxygen treated 0.1-g HY zeolite (a), the zeolite reacted with 6.65 hPa (5 Torr) $PhSiH_3$ at 423 K for 2 h then evacuated at the same temperature for 30 min (b), and the zeolite after extracting polysilanes in hexane (c). The spectra were recorded at 298 K.

298 K followed by evacuation at the same temperature in Figures 3, 4, and 5, while it was reacted with $PhSiH_3$ molecules at the pressure of 6.65 hPa (5.0 Torr) at 423 K for 2 h in Figures 7 and 8. Therefore, in this reaction, $PhSiH_3$ molecules can react with the grafted $[O]_{2-3}-SiH_x$ species and the further Si length prolongation reaction will be expected. In HY zeolite, both the hydroxyl groups in the supercages and in the sodalite cages are observed at around 3600−3650 cm^{-1} and 3530−3580 cm^{-1}, in addition to silanol groups at 3740 cm^{-1}.[76−78] In our HNaY zeolite with a protonic exchange of 68%, relatively few hydroxyl groups should be located in the sodalite cages since hydroxyl groups in supercages are bridging groups and work as strongest acid sites. The hydroxyl groups in Figure 8 are peaked at 3620 and 3680 cm^{-1}. The latter wavenumbers (3680 cm^{-1}) are very similar (3675 cm^{-1}) to those observed on the Y zeolite treated with stream whose extraframework aluminum was partially removed with aqueous HCl.[79] The hydroxyl groups detected at 3680 cm^{-1} in our samples can be assigned to those in supercages. Therefore, the result in Figure 8 implies that SiH_x species are grafted only to supercages and that in Figure 7 may suggest the Si−Si bond formation reaction. According to the discussion mentioned above, the initial sticking Si−H species on the zeolite framework at 2210 and 2260 cm^{-1} can be assigned

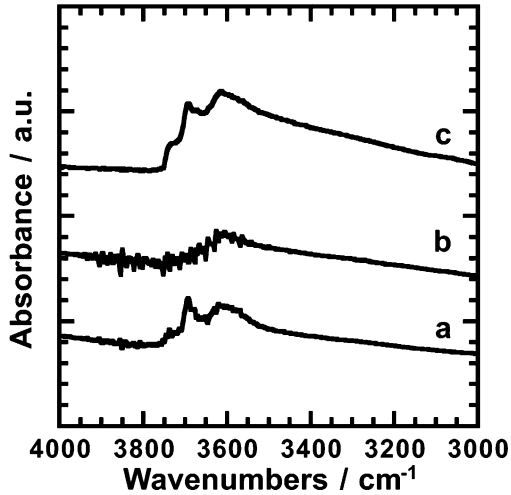

Figure 8. Infrared spectra of O−H stretching frequency region on the 0.1-g HY zeolite. The symbols a, b, and c are the same as in Figure 6. The spectra were recorded at 298 K.

to $[O]_2-SiH_2$ and $[O]_3-SiH$, respectively. Whereas the $[O]_2-SiH_2$ species is stable even at 473 K in Figure 5, it can be converted to the $[O]_3-SiH$ species at 523 K. Therefore the species at 2260 cm^{-1} in Figure 7 is different from the grafted $[O]_3-SiH$ species. It is expected that the successive Si−Si formation reaction will occur as follows. Considering the reaction temperature at 423 K, reaction 4 will be most probable. It is noted that some terminated hydrogen atoms will be replaced by phenyl groups as mentioned below

$$[O]-SiH_3 + n\mathrm{PhSiH_3} \rightarrow [O]-(SiH_2)_n-SiH_3\,[I] + n\mathrm{Ph-H} \quad (3)$$

$$2[O]-SiH_3 + n\mathrm{PhSiH_3} \rightarrow [O]_2-SiH-(SiH_2)_{n-1}-SiH_3\,[II] + n\mathrm{Ph-H} + SiH_4 \quad (4)$$

$$3[O]-SiH_3 + n\mathrm{PhSiH_3} \rightarrow [O]_3-Si-(SiH_2)_{n-1}-SiH_3\,[III] + n\mathrm{Ph-H} + 2SiH_4 \quad (5)$$

In the reaction 4, $[O]_2-SiH_2$ species are formed from $[O]-SiH_3$ species as shown in the reaction 2 and SiH_4 should be formed during the process. The formed silane molecules can participate in the polymerization to yield polysilanes. The Si−H stretching frequencies of nonoxidized SiH_3 as well as nonoxidized $SiPhH_2$ species should be observed below 2150 cm^{-1}. However, these species could not be detected, but oxygen-terminated polysilanes will be formed. Hydrogen desorbs from polysilane compounds at 573 K.[80] On the other hand, hydrogen desorbs from dihydride and monohydride on Si single crystals at about 680 and 800 K, respectively.[81] These facts imply that the hydrogen abstraction is more facile on polysilanes and such the abstraction will be the trigger to the subsequent propagation reaction. It is suggested that hydrogen-terminated species in zeolite pores resembles polysilane families, whereas they are grafted to zeolite framework.

Silicon 2p XPS spectra of the zeolite and the $PhSiH_3$-reacted zeolite are shown in Figure 6. Phenylsilane was reacted at 423 K overnight, and the reaction was repeated 4 times by dosing new $PhSiH_3$ molecules to the zeolite. Binding energy values were referenced to C 1s at 284.4 eV, then O 1s values were 531.6 eV. These values are the same as those repoted in NaY zeolite.[82] Although the intensity of the O 1s XPS signal decreased to about 80% after the reaction with $PhSiH_3$, the Si 2p intensity increased to about 20% as shown in Figure 6. The

difference spectrum in Figure 6 corresponds to the increase of Si species formed in the zeolite supercages. The two components can be deconvoluted at 101.4 and 102.3 eV. Phenylsilane plasma polymers with silicon networks show Si 2p XPS signals peaked at 100.9−101.5 eV, depending on the polymerization temperature.[83] Tertially butyl substituted organosilicon nanocluster ($Si_1C_{1.19}H_{3.07}O_{0.07}$) shows the Si 2p peak at about 100 eV with a shoulder at 102 eV.[84] While a network polysilane, poly(alkylsilyne), shows the Si 2p peak at 102.6 eV.[85] Therefore, it will be reasonable to assign the Si species detected in our experiments at 101.4 and 102.3 eV as polysilane families. Considering that the SiO_2/Al_2O_3 ratio is 5.6 and the unit cell of Y-type zeolite is composed of 192 Si or Al ions,[36] about 30 Si atoms (20% of 142 Si atoms) should be increased as polysilane families in the zeolite supercage. The atomic ratio of C to O increased on the $PhSiH_3$-reacted zeolite (0.07 to 0.20) so that the formed polysilanes will contain partial phenyl groups as terminated groups. Since the C to Si atomic ratio is below 1, less than one phenyl group should be present per 6 Si backbone atoms in the polysilanes on the $PhSiH_3$ reacted zeolite. The Si 2p signal can be detected at 98 eV on the $PhSiH_3$ reacted zeolite. This species will be negatively charged Si clusters formed from SiH_4 in the reactions 4 and 5. These species have been observed on $AlPO_4$-5 molecular sieves.[86]

Extraction of chained Si species formed in zeolite supercages into organic solvent was carried out. As shown in Figure 7, SiH_x species disappeared after extracting the $PhSiH_3$-reacted zeolite with hexane. Extracted species show the characteristic PL spectrum at 298 K, which is discussed in the next section. Hydroxyl groups are rejuvenated after they are dipped in water-free hexane as shown in Figure 8. If such hydroxyl groups rejuvenation occurs by the rection with trace amount of water in the air or in hexane solution, the broad hydrogen-bonded species should be observed at around 3400 cm^{-1}. No hydroxyl group was detected after the polysilane-anchored zeolite sample was exposed to air for awhile at 298 K. The fact suggests that the rejuvenation will probably be caused by the hydrogen abstraction from the zeolite anchored polysilane species and olefinic polysilanes will be solvated in hexane as follows

$$[O]-(SiH_2)_n-SiH_3\ [I] \rightarrow [O]-H + Si_{n+1}H_{2n+2} \quad (6)$$

$$[O]_2-SiH-(SiH_2)_{n-1}-SiH_3\ [II] \rightarrow 2[O]-H + Si_{n+1}H_{2n} \quad (7)$$

$$[O]_3-Si-(SiH_2)_{n-1}-SiH_3\ [III] \rightarrow 3[O]-H + Si_{n+1}H_{2n-2} \quad (8)$$

PL spectra of the Si species synthesized in zeolite supercages were studied. PL spectra of zeolite, the polysilanes in zeolite supercages, and those extracted in hexane solution are shown in Figure 9. For comparison, the PL spectrum of $PhSiH_3$ is also shown, whereas the intensity is very weak. It is noted that a band-path filter was used for PL spectra to cut out the excitataion wavelength at 266 nm. Therefore, PL spectra of polysilanes extracted in hexane solution and $PhSiH_3$ are not symmetrical and the high-energy side above 4.2 eV is partly removed. The effect of the band-path filter on PL spectra is detected clearly at the PL shoulder observed at $PhSiH_3$. Therefore, the filter does not effect influence on the PL peak positions. The extracted polysilanes shows a similar PL with $PhSiH_3$, but the PL intensity is very intense and the peak energy shifts significantly from 4.15 to 4.07 eV (redshift). The reflection of laser excitation at 266 nm is responsible for a sharp spike at 4.66 eV. The sharp

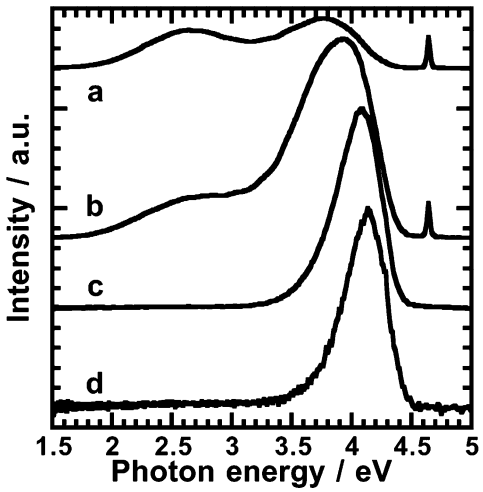

Figure 9. PL spectra of the 1013-hPa oxygen-treated zeolite (a), the zeolite reacted with 6.65 hPa $PhSiH_3$ at 423 K for 2 h (b), polysilanes extracted in hexane (c), and $PhSiH_3$ in hexane (d). PL spectra of zeolite samples and solutions were recorded at 298 K under vacuum and in air, respectively.

spike at 266 nm was too strong in PL spectra on the zeolite by the reflection to be cut out completely. The spike was observed in zeolite and polysilanes in zeolite pores. As mentioned before, the zeolite has two PL peaks at 2.7 and 3.6 eV even after oxidation at 573 K. The PL spectrum of polysilanes in zeolite cages seems to be composed of a PL component near 4 eV in addition to two components in the zeolite. On the other hand, polysilanes extracted in hexane solution have a sharp PL component peaked at 4.07 eV. Organosilicon polymers show various PL bands. Dihexylpolysilane, polyhexylsilane with planar structure, polysilane, polysilane alloy, and amorphous silicon show PL peaked at 3.2, 2.9, 2.5, 1.2, and 0.8 eV, respectively.[87] *syn*-Tricyclooctane molecules with ladder structures show a luminescence peaked at 2.25 eV.[88] Layer-structured polysilanes show optical absorption spectra after annealing at different temperature, that is, band-gap energy changes from about 2.5 to 1.1 eV.[89] PL in two-dimensional σ-conjugated organosilicon polymers such as polysilylenes and layered polysilanes have also been observed at 3.3−2.3 eV.[90,91] Normally, alkyl-substituited polysilanes show PL spectra with peak energies below 3.7 eV.[1] When the substituents are diphenyl groups in polysilanes, the PL peak energy drastically decreases to 3.1 eV.[92] The PL energy corresponding to the difference between the HOMO and LUMO of polysilanes in our system is larger than these compounds.

Figure 10 shows UV absorption spectra of polysilanes extracted from zeolite pores into hexane, in addition to benzene and $PhSiH_3$. Nothing was extracted in hexane from oxygen-treated zeolites. Benzene shows a characteristic broad UV absorption peak centered at 250 nm. On the other hand, $PhSiH_3$ shows the separated UV peaks at 271, 265, 260, 254, and 248 nm due to the phenyl group. Both benzene and $PhSiH_3$ show the intense UV peaks due to the phenyl group because of the extremely high absorption coefficient. Although the UV spectrum of polysilanes extracted from zeolite pores shows some peaks similar to $PhSiH_3$, they shift to higher wavelength by about 10−20 nm (red shift). Trace amount of polysilanes formed in the zeolite pores will be partially terminated with phenyl groups as suggested in XPS results. Most significantly, a broad signal was detected in the extracted species at around 220−280 nm. Absorption peak energies of polysilanes strongly depend on the backbone structure.[12] Therefore, the broad signal

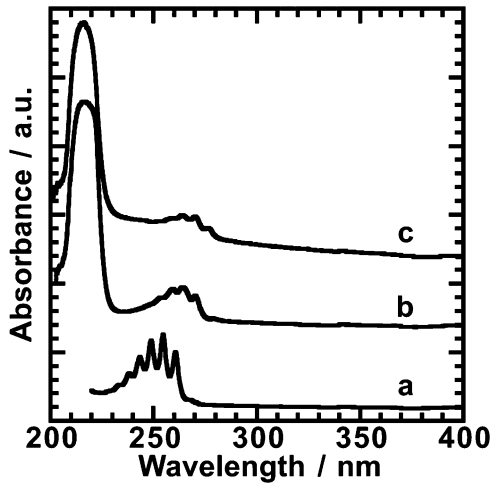

Figure 10. UV absorption spectra of benzene (a), $PhSiH_3$ (b), and polysilanes extracted from zeolite (c). All samples were diluted in hexane.

will be associated with the backbone structure of polysilanes synthesized in the zeolite supercages. In general, polysilanes terminated with methyl groups are insoluble in organic solvents although those with phenyl groups are soluble.[93] Phenylsilane molecules can be evacuated at 423 K as shown in Figure 5, and no C−H (phenyl) group was detected in IR spectra after evacuating the reacted zeolite at 423 K. However, the detection limit of IR (10^{-6} mol) is much less than XPS (0.01 surface monolayer). Therefore, it is reasonable to consider the possibility of phenyl group terminated polysilanes in our system. In addition, polysilanes in our system will be olefinic by the hydrogen abstraction as shown in eqs 7 and 8 and, as a result, will be soluble in organic solvent.

The polysilanes structure changes with the temperature and their PL peaks shift to higher energies as the structure changes from trans helix to amorphous.[94] Polysilanes exhibits the intense near-UV absorption bands attributed to the transitions between σ-delocalized Si−Si bonding HOMOs and antibonding LUMOs.[95,96] The wavelength of the absorption band increases almost linearly from 200 to 300 nm as a function of the chain length until $n = 10$ for $(dialkylsilylene)_n$.[96] Then, the broad UV absorption at around 220−280 nm observed in our polysilanes imply the energy gaps between the HOMO and LUMO of the polysilanes, which corresponds to 4.4−5.6 eV. The emission mechanism in organosilanes has been ascribed as the Si−Si $\sigma^*-\sigma$ de-excitation.[95] The Stokes shift between the absorption peak energy and the luminescence peak energy increases with increases in the width of absorption spectra ΔE in many polysilanes[12] to be near the value of $0.7\Delta E$.[92] According to our results, the width of absorption spectra due to the backbone structure reaches more than 1.2 eV. If such the relation can be applied to our system, the Stokes shift should be about 0.8 eV. Whereas the polysilanes formed in the zeolite supercages show the PL peaked at 4.07 eV, PL spectra in our system are excited at 266 nm (4.66 eV). Then, the Stokes shift will be estimated to be 0.6 eV (4.66−4.07), however, the real shift cannot be measured exactly. The wide distribution of ΔE will also originate from the effect of the spatial inhomogenity on the backbone chain structures or lengths.

Conclusions

In the present study, the synthesis of chained Si species in the zeolite pores was tried by the step-by-step reactions using $PhSiH_3$. The initial grafting reaction and the propagation process were studied with TPD experiments and IR spectra. The formed Si species were characterized with XPS. They could be extracted in hexane solution, and the extracted species were characterized with UV and PL. Conclusions are as follows.

(1) The initial grafting of Si species to zeolite framework using $PhSiH_3$ selectively proceeds on the supercage OH groups, which yields $[O]-SiH_3$ species even at 298 K. Adsorbed $[O]-SiH_3$ species change into $[O]_2-SiH_2$ and finally to $[O]_3-SiH$ species at elevated temperatures.

(2) The adsorbed $[O]-SiH_3$ species are stable at 473 K under evacuation. However, in the presence of $PhSiH_3$ molecules they can react with another $PhSiH_3$ molecules at 473 K and they will be most probably changed into $[O]_2-SiH-(SiH_2)_{n-1}-SiH_3$ species. The stretching frequency of Si−H species supports the formation of linear polysilanes attached to zeolite framework.

(3) The polysilanes formed in zeolite supercages show Si 2p XPS signals peaked at 101.4 and 102.3 eV. The XPS quantiative analysis suggests that the polysilane families are composed of of about 30 network Si atoms with some carbon atoms probably as phenyl groups.

(4) The polysilanes formed in zeolite supercages show intense PL spectra peaked at around 4 eV. They can be extracted in hexane solution. The extracted polysilanes show PL peaked at 4.07 eV, which is redshifted compared to PL of $PhSiH_3$ at 4.15 eV. The extracted polysilanes will have phenyl groups, which will be responsible for the solubility in organic solvents.

(5) The polysilanes extracted in hexane show the characteristic broad UV absorption ranging from 220 to 280 nm. They will be assigned to the transitions from HOMOs to LUMOs of Si−Si $\sigma^*-\sigma$ de-excitation in the backbone structure of polysilanes. The wide distribution of absorption energies in the polysilanes synthesized in zeolite supercages will be effected by the inhomogenity of backbone structures and lengths.

References and Notes

(1) Miller, R. D.; Michl, J. *Chem. Rev.* **1989**, *89*, 1359.
(2) Canham, L. T. *Appl. Phys. Lett*. **1990**, *57*, 10, 46.
(3) Maeda, Y.; Tsukamoto, N.; Yazawa, Y.; Kanemitsu, Y.; Matsumoto, Y. *Appl. Phys. Lett*. **1991**, *59*, 3168.
(4) Wilson, W. L.; Szajowski, P. F.; Brus, L. E. *Science* **1993**, *262*, 1242.
(5) Schuppler, S.; Friedman, S. L.; Marcus, M. A. *Phys. Rev. B* **1995**, *52*, 4910.
(6) Carlos, W. E.; Prokes, S. M. *J. Vac. Sci. Technol*. **1995**, *13*, 1653.
(7) Kanemitsu, Y. *Phys. Rev. B* **1996**, *53*, 13515.
(8) Shimasaki, M.; Show, Y.; Iwase, M.; Izumi, T.; Ichinose, T.; Nozaki, S.; Morisaki, H. *Appl. Surf. Sci*. **1996**, *92*. 617.
(9) Hayashi, S.; Kanazawa, Y.; Kataoka, M.; Nagarede, T.; Yamamoto, K. *Z. Phys. D* **1993**, *26*, 144.
(10) Takagi, H.; Ogawa, H.; Yamazaki, Y.; Ishizaki, A.; Nakagiri, T. *Appl. Phys. Lett*. **1990**, *56*, 2379.
(11) Kanemitsu, Y.; Ogawa, H.; Shiraishi, K.; Takeda, K. *Phys. Rev. B* **1993**, *58*, 4883.
(12) Koshida, N.; Matsumoto, N. *Mater. Sci. Eng. R.* **2003**, *40*, 169.
(13) Jarrold, M. A. *Science* **1991**, *252*, 1085−1092.
(14) Okada, R.; Iijima, S. *Appl. Phys. Lett*. **1991**, *58*, 1662.
(15) Jarrold, M. F.; Ray, U.; Creegan, K. M. *J. Chem. Phys*. **1990**, *93*, 224.
(16) Goldstein, A. N. *Appl. Phys. A* **1996**, *62*, 33.
(17) Jarrold, M. F.; Honea, E. C. *J. Am. Chem. Soc*. **1992**, *114*, 459.
(18) Choo, C.-K.; Sakamoto, T.; Tanaka, K.; Nakata, R. *Appl. Sur. Sci*. **1999**, *148*, 116.
(19) Choo, C.-K.; Sakamoto, T.; Tohara, M.; Tanaka, K.; Nakata, R.; Okuyama, N. *Surf. Sci*. **2000**, *445*, 480.
(20) Nozue, Y.; Kodaira, T.; Goto, T. *Phys. Rev. Lett*. **1992**, *68*, 3789.
(21) Nozue, Y. *J. Jpn. Phys. Soc.* **1993**, *48*, 624.
(22) Tamura, K.; Hosokawa, S.; Endo, H.; Yamasaki, S.; Oyanagi, H. *J. Phys. Soc. Jap*. **1986**, *55*, 528.
(23) Parise, J. B.; MacDougall, J. E.; Herron, N.; Farlee, R.; Sleight, A. W.; Wang, Y.; Bein, T.; Moller, K.; Moroney, L. M. *Inorg. Chem*. **1988**, *27*, 221−228.
(24) Nozue, Y. *Solid Phys.* **1991**, *26*, 367.

(25) Wang, Y.; Herron, N. *J. Phys. Chem*. **1988**, *92*, 4988.
(26) Stramel, R. D.; Nakamura, T.; Thomas, J. K. *J. Chem Soc., Faraday Trans. 1* **1988**, *84*, 1287.
(27) Herron, N.; Wang, Y.; Eddy, M. M.; Stucky, G. D.; Cox, D. E.; Moller, K.; Bein, T. *J. Am. Chem. Soc*. **1989**, *111*, 530.
(28) Fox, M. A.; Pettit, T. L. *Langmuir* **1989**, *5*, 1056.
(29) Stucky, G. D.; MacDougall, J. M. *Science* **1990**, *247*, 669.
(30) MacDougall, J. E.; Eckert, H.; Stucky, G. D. *J. Am. Chem. Soc*. **1989**, *111*, 8006.
(31) Cox, S. D.; Gier, T. E.; Stucky, G. D.; Bierlein, J. *J. Am. Chem. Soc*. **1988**, *110*, 2986.
(32) Wu, C.-G.; Bein, T. *Science* **1994**, *264*, 1757.
(33) Wu, C.-G.; Bein, T. *Science* **1994**, *266*, 1013.
(34) Howe, R. F. *Tailored Metal Catalysts*; Iwasawa, Y. D., Ed.; Reidel: Dordrecht, 1986; p 141.
(35) Ichikawa, M. *Tailored Metal Catalysts*; Iwasawa, Y. D., Ed.; Reidel: Dordrecht, 1986; p 183.
(36) Meier, W. M.; Olson, D. H. *Atlas of Zeolite Structure Types*, revised ed.; Butterworth-Heinemann: Boston, 1992.
(37) Feng, S.; Bein, T. *Nature* **1994**, *368*, 834.
(38) Tsikoyiannis, J. G.; Haag, W. O. *Zeolites* **1992**, *12*, 126.
(39) Geus, E. R.; den Exter, M. J.; van Bekkum, H. *J. Chem. Soc., Chem Comm*. **1992**, *88*, 3101.
(40) Ozin, G. A.; Kuperman, A.; Stein, A. Angew. *Chem. Int. Ed. Engl*. **1989**, *28*, 359.
(41) Kasai, P. *J. Phys. Chem*. **1965**, *43*, 3322.
(42) Harrison, M. R.; Edwards, P. P.; Klinowski, J.; Thomas, J. M. *J. Solid State Chem*. **1984**, *54*, 330.
(43) Sun, T.; Seff, K.; Heo, N. H.; Petranovskii, V. P. *Science* **1993**, *259*, 495.
(44) Olson, D. H. *J. Phys. Chem*. **1970**, *74*, 2758.
(45) Fitch, A. N.; Jovic, H.; Renouprez, A. *J. Phys. Chem.* **1986**, *90*, 1311.
(46) Srdanov, V. I.; Haug, K.; Metiu, H.; Stucky, G. D. *J. Phys. Chem*. **1992**, *96*, 9039.
(47) Launois, P.; Moret, R.; Bolloc'h, D. Le.; Albouy, P. A.; Tang, Z. K.; Li, G.; Chen, J. *Solid State Commun*. **2000**, *116*, 99.
(48) Werner, L.; Caro, J.; Finger, G.; Kornatoski, J. *Zeolites* **1992**, *12*, 658.
(49) Bein, T. Supramolecular Architecture. *ACS Symposium Series 499*; Bein. T., Ed.; American Chemical Society: Washington, DC, 1992; Chapter 20.
(50) Choo, C.-K.; Sakamoto, T.; Tanaka, K.; Nakata, R.; Asakawa, T. *Appl. Surf. Sci*. **1999**, *140*, 126.
(51) Choo, C.-K.; Sakamoto, T.; Tanaka, K.; Nakata. *Appl. Surf. Sci*. **1999**, *148*, 116.
(52) Choo, C.-K.; Sakamoto, T.; Tohara, M.; Tanaka, K.; Nakata, R.; Okuyama, N. *Surf. Sci*. **2000**, *445*, 480.
(53) Ozin, G. A.; Dag, O.; Kuperman, A.; Macdonald, P. M. *Stud. Surf. Sci. Catal*. **1994**, *84*, 1107.
(54) Chomski, E.; Dag, G.; Kuperman, A.; Coombs, N.; Ozin, G. A. *Chem. Vap. Deposition* **1996**, *2*, 8.
(55) He, J.; Klug, D. D.; Tse, J. S.; Ratcliffe, C. I.; Preston, K. F, *Appl. Phys. Lett*. **1997**, *71*, 3194.
(56) He, J.; Ba, Y.; Ratcliffe, C. I.; Ripmeester, J. A.; Klug, D. D.; Tse, J. S. *Appl. Phys. Lett*. **1999**, *74*, 830.
(57) Glinka, Yu. D.; Lin, S.-H.; Hwang, L.-P.; Chen, Y.-T. *J. Phys. Chem. B* **2000**, *104*, 8562.
(58) Glinka, Yu. D.; Lin, S.-H.; Chen, Y.-T. *Appl. Phys. Lett*. **1999**, *75*, 778.
(59) Glinka, Yu. D.; Lin, S.-H.; Chen, Y.-T. *Phys. Rev. B* **2000**, *62*, 4733.
(60) Itoh, C.; Tanimura, K.; Itoh, M.; Itoh, N. *Phys. Rev. B* **1989**, *39*, 11183.
(61) Glinka, Yu. D.; Lin, S.-H.; Hwang, L.-P.; Chen, Y.-T. *J. Phys. Chem. B* **2000**, *104*, 8562.
(62) Fitch, A. N.; Jobic, H.; Renouprez, A. *J. Phys. Chem*. **1986**, *90*, 1311.
(63) Su, B.-L. *J. Chem. Soc., Faraday Trans*. **1997**, *93*, 1449.
(64) Jobic, H.; Fitch, A. N.; Combet, J. *J. Phys. Chem. B* **2000**, *104*, 8491.
(65) Beck, L. W.; Xu, T.; Nicholas, J. B.; Haw, J. F. *J. Am. Chem. Soc*. **1995**, *117*, 11594.
(66) Schmidt, J.; Stuhlmann, Ch.; Ibach, H. *Surf. Sci*. **1994**, *302*, 10.
(67) Gupta, P.; Dillon, A. C.; Bracker, A. S.; George, S. M. *Surf. Sci*. **1991**, *245*, 360.
(68) Tsu, D. V.; Lucovsky, G.; Davidson, B. N. *Phys. Rev. B* **1989**, *40*, 1795.
(69) Glass, J. A., Jr.; Edward, A.; Wovchko, A.; Yates, J. T., Jr. *Surf. Sci*. **1995**, *338*, 125.
(70) Parsons, G. N.; Lucovsky, G. *Phys. Rev. B* **1990**, *41*, 1664.
(71) Kato, Y.; Ito, T.; Hiraki, A. *Jpn. J. Appl. Phys*. **1988**, *27*, L1406.
(72) Morrison, P. W., Jr.; Haigis, J. R. *J. Vac. Sci. Technol. A* **1993**, *11*, 490.
(73) Ogata, Y.; Niki, H.; Sakka, T.; Iwasaki, M. *J. Electrochem. Soc*. **1995**, *142*, 195.
(74) Han, S. M.; Aydil, E. S. *J. Vac. Sci. Technol. A* **1996**, *14*, 2062.
(75) Steele, M. R.; Macdonald, P. M.; Ozin, G. A, *J. Am. Chem. Soc*. **1993**, *115*, 7285.
(76) White, J. L.; Jelli, A. N.; Andre, J. M.; Fripiat, J. J. *Trans. Faraday, Soc*. **1967**, *63*, 461.
(77) Olson, D. H.; Dempsey, E. *J. Catal*. **1969**, *13*, 221.
(78) Mortier, W. J.; Jacobs, P. A. *Zeolites* **1982**, *2*, 226.
(79) Cairon, O.; Chevreau, T.; Lavalley, J. C, *J. Chem. Soc., Faraday Trans*. **1998**, *91*, 3039.
(80) He, J.; Tse, J. S.; Klug, D. D.; Preston, K. F. *J. Mater. Chem*. **1998**, *8*, 705.
(81) Gupta, P.; Colvin, V. L.; George, S. M. *Phys. Rev*. **1988**, *37*, 8234.
(82) Barr, T. L. *Practical Surface Anbalysis by Auger and X-ray Photoelectron Spectroscopy*, 1st ed.; Briggs, D., Seah, M. P., Ed.; John & Miley: Chichester, 1984; p 330.
(83) Oelhafen, P.; Cutro, J. A.; Haller, I. *J. Electctron Spectrosc. Relat. Phenom.* **1984**, *34*, 105.
(84) Watanabe, A.; Fujitsuka, M.; Ito, O. *Thin Solid Films* **1999**, *354*, 13.
(85) Watanabe, A.; Nagai, Y.; Matsuda, M. *Jpn. J. Appl. Phys.* **1995**, *34*, L452.
(86) Choo, C.-K.; Sakamoto, T.; Tanaka, K.; Nakata, R.; Asakawa, T. *Appl. Surf. Sci*. **1999**, *140*, 126.
(87) Furukawa, K.; Fujino, M.; Matsumoto, N. *Macromolecules* **1991**, *24*, 3432.
(88) Kanemitsu, Y.; Suzuki, K.; Kyusin, S.; Matsumoto, H. *Phys. Rev. B* **1995**, *51*, 10666.
(89) Kawaji, H.; Yamanaka, S.; Shiotani, M. *Hyomen Kagaku* **1997**, *7*, 149.
(90) Wilson, W. L.; Weidman, T. W. *J. Phys. Chem*. **1991**, *95*, 4568.
(91) He, J.; Tse, J. S.; Klug, D. D.; Preston, K. F. *J. Meter. Chem*. **1998**, *8*, 705.
(92) Takeda, K.; Teramae, H.; Matsumoto, N. *J. Am. Chem. Soc*. **1986**, *108*, 8186.
(93) Matsumoto, N. *Nihon Butsuri Gakkaishi* **1992**, *47*, 632.
(94) Tanaka, K.; Komatsu, Y.; Hamaguchi, K.; Choo, C.-K.; Nakata, R. In preparation.
(95) Tokura, Y.; Tachibana, H. *Ohyou Butsuri* **1991**, *60*, 990.
(96) West, R. Organopolysilanes. In *Comprehensive Organometallic Chemistry*; Abel. E., Ed.; Pergamon: Oxford, England, 1982; Chapter 9.4, pp 365−397.
(97) West, R. *J. Organomet. Chem*. **1986**, *300*, 327.